Magnetic nanobraids of iron-doped amorphous silica

Yu, M. B.; Xiong, Y. Z.; Chen, J. S.; Xu, Chunxiang; Sun, Xiaowei; Dong, Zhili

2004

Xu, C., Sun, X., Yu, M. B., Xiong, Y. Z., Dong, Z. L. & Chen, J. S. (2004). Magnetic nanobraids of iron-doped amorphous silica. Applied Physics Letters, 85 (22), 5364-5366.

https://hdl.handle.net/10356/93777

https://doi.org/10.1063/1.1830686

APPLIED PHYSICS LETTERS VOLUME 85, NUMBER 22 29 NOVEMBER 2004

Magnetic nanobraids of iron-doped amorphous silica

C. X. Xu and X. W. Sun[a)]
School of Electric and Electronic Engineering, Nanyang Technological University, Nanyang Avenue, Singapore 639798, Singapore

M. B. Yu and Yong Zhong Xiong
Institute of Microelectronics, 11 Science Park Road, Singapore Science Park II, Singapore 117684, Singapore

Z. L. Dong
School of Materials Engineering, Nanyang Technological University, Nanyang Avenue, Singapore 639798, Singapore

J. S. Chen
Data Storage Institute, 5 Engineering Drive 1, Singapore 117684, Singapore

(Received 21 June 2004; accepted 12 October 2004)

Using silicon, iron oxide, and graphite powders as source materials, braid-like nanostructures of iron-doped amorphous silica were fabricated by vapor-phase transport. Each braid was composed of a bunch of entangled nanowires with uniform size. The formation of the nanobraids was mainly due to simultaneous nucleation in a vapor–liquid–solid process. Magnetic measurement showed that the iron-doped silica nanobraids were ferromagnetic at room temperature. © *2004 American Institute of Physics*. [DOI: 10.1063/1.1830686]

Since the report of carbon nanotube,[1] fabrication and characterization of one-dimensional (1D) nanomaterials have been investigated intensively because of their unique properties associated with size reduction in two dimensions, yet maintaining easy manipulation with microscale in the other dimension. Various kinds of metals, semiconductors, and insulators in 1D form have been synthesized.[1–8] Among them, silica nanowire[8–11] has attracted great interest-because of its intense and stable blue photoluminescence, promising for applications in high-resolution optical heads of a near-field optical microscopy and interconnections for integrated optical devices. So far, various fabrication methods have been employed, such as thermal evaporation and laser ablation using Si, SiO_2, and SiC as source materials.[8–11] In these methods, oxygen was generally used as carrier gas, and gold and iron particles were used as catalysts. Recently, some aesthetic nanostructures of silica with springlike, fishbonelike, gourdlike, spindlelike, badmintonlike, and octopuslike morphologies were prepared by the chemical vapor deposition of silane with molten gallium as the catalyst.[12,13]

On the other hand, magnetic materials are the most widespread and competitive information carriers for data recording. Magnetic nanomaterials are considered to be the most promising candidates for information storage and spintronic devices because of the possibility to exploit the effect of quantum tunneling of magnetization.[14–16] Introducing cobalt, nickel, and iron into silica host, magnetic thin films,[17] nanoparticles,[18] and nanocomposites[15,19] have been obtained. In this letter, we shall present the fabrication of iron doped amorphous silica in nanobraids form and their magnetic properties.

The fabrication of silica nanobraids is based on a vapor–phase transport approach, which has been reported previously.[6,20] The mixture of silicon, iron oxide, and graphite powder was used as source material. The fabrication was performed in a one-end-sealed quartz tube which was placed in a tube furnace at 1150 °C. After sintering for 1 h, a layer of white products were obtained on a slice of silicon at downstream area with lower temperature (900–1000 °C). The entire procedure was carried out in air. After fabrication, the scanning electron microscopy (SEM) was employed to examine the morphology of the product. The crystal structure of the sample was characterized by x-ray diffraction (XRD) using Cu $K_{\alpha 1}$ radiation. A JEOL 3010 high-resolution transmission electron microscope operated at 300 kV was employed to detect the lattice structure. The energy-dispersive x-ray spectroscope (EDX) attached to the transparent electron microscope (TEM) was employed to detect the chemical composition. The magnetic properties of the nanobraids were measured by a vibrating sample magnetometer (VSM) at room temperature.

Figure 1 shows the SEM images of the nanostructures

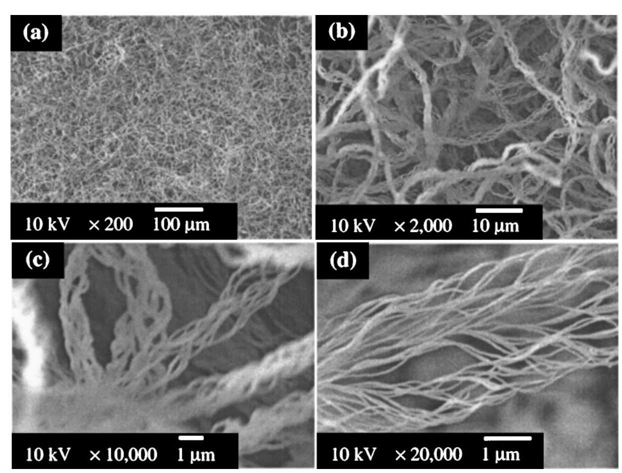

FIG. 1. SEM images of the silica nanobraids with low (a), medium (b), and high (c), and (d) magnifications.

a)Author to whom correspondence should be addressed; electronic mail: exwsun@ntu.edu.sg

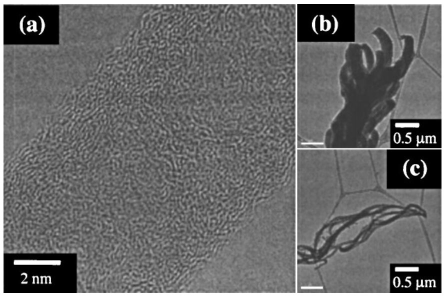

FIG. 2. TEM images of the silica nanobraids. (a) high resolution TEM image of an individual nanowire; (b) a typical morphology of the entangling nanowires; and (c) a strand of nanobraids formed by branching nanowires.

with various magnifications. It can be seen from Fig. 1(a) that a dense layer of nanowires is covered on the substrate. With increased magnification, Fig. 1(b) shows that these nanowires entwine each other to form numerous bunches of braids with diameters of 1–2 μm. It is worth mentioning that the yield of nanobraids is high. Figures 1(c) and 1(d) show more detailed SEM image of the nanobraids. Most of the nanobraids are composed of about ten nanowires, and some of them have less than 5 or more than 20 nanowires. The nanowires themselves have uniform size of about 30 nm in diameter and several hundred microns in length.

The x-ray diffraction (XRD) and high resolution TEM were employed to analyze the crystallization of the nanobraids. No diffraction peak was observed in the XRD pattern (not present here). This indicates the amorphous state of the SiO_x nanobraids. Figure 2(a) shows the high resolution TEM image of a silica nanowire with more insightful information, proving directly the amorphous phase of the nanowire. Figure 2(b) shows the end of a strand of nanobraids with relatively flat surface. Figure 2(c) shows a few nanowires sharing the same base to form a strand of nanobraids.

Figure 3 shows the EDX spectrum of the nanobraids showing in Fig. 2(b). It can be seen from Fig. 3 that, strong signals of Si and O appear in the EDX spectrum while two weak peaks from iron can also be observed. The copper signal originated from the copper grid supporting the TEM sample. The carbon signal was caused by some carbon contamination during sample handling and preparation of TEM sample. This indicates that the nanobraids are composed of silicon oxide doped with iron. It is worth mentioning that there might be a cobalt signal overlapping with one of the iron peak. The cobalt signal, if any, is probably originated

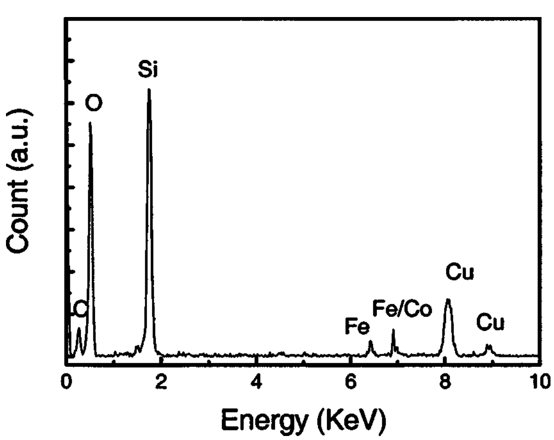

FIG. 3. EDX spectrum of the silica nanobraids shown in Fig. 2(b).

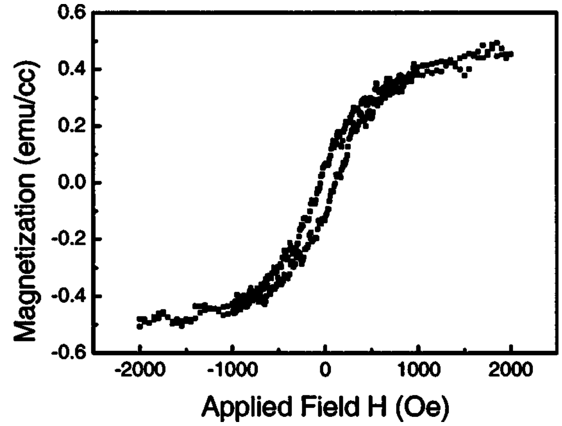

FIG. 4. Magnetization **M** vs applied magnetic field **H** curve detected at room temperature.

from either the source material of iron oxide or the TEM sample holder. The quantitative analysis of EDX demonstrates that the element ratio of Si–O is about 1:1.4, and the iron content is about 3.2 at. %. It should be mentioned that this iron concentration obtained here may not be exact. It is just an indication of iron incorporated into the nanobraids.

The vapor–liquid–solid (VLS) mechanism[10,11] is generally used to explain the growth process of nanowires. The typical feature of VLS process is the existence of a catalyst nanoparticle at the top of the nanowire. In the present case, the catalysts should originate from the thermal carbon reduction of iron oxide. However, the tops of the nanowires are almost flat, as shown TEM image in Fig. 2(b). The EDX signal of iron can still be observed at the ends of the nanowires although no iron nanoparticles can been identified at the top of the nanowires. This indicates that iron did not only act as catalyst but also possibly diffuse into the bodies of the SiO_x nanowires in the growth. The EDX detected at the other segments further confirmed that the iron was doped into whole nanowires. The source vapor generated from the high temperature region is transferred to the substrate area to form liquid Fe–Si–O alloy droplets. When the liquid becomes supersaturated with Si and O atoms, the recrystallization of the atomic Si–O species is prevented, resulting in the formation of amorphous silica.[21] The formation of the nanobraids involves two phenomena—branching growth and simultaneous nucleation.[13] The branching growth means that one nanowire splits into several branches when new catalysts deposited on the trunk to form polycentric nuclei.[10] In this case, the morphology shows a small head and big tail structure as shown in Fig. 2(c). However, the branching structure is seldom observed in our samples. Mostly, each braid shows a uniform thickness because different parts comprise almost the same amount nanowires [see Fig. 1(b)]. This indicates that many nanowires simultaneously nucleated and then jointly grew at nearly the same rate. During the bunch formation, Van der Waals interactions might provide the basic force to make the adjacent nanowires entangling together.[11]

Figure 4 shows the relationship of the magnetization **M** versus the applied magnetic field **H** for the iron-doped silica nanobraids by VSM method. In the magnetic measurement, the applied field was parallel to the silicon substrate that was used to collect the silica nanobraids. With a random orientation of the nanobraids on silicon substrate (Fig. 1), the direction of the nanobraids is random with respect to the applied field in the measurement. Although the iron content in the nanobraids is low, a clear hysteresis loop can be observed, indicating the nanobraids are ferromagnetic. From the **M**-**H** curve in Fig. 4, the saturation magnetization $\mathbf{M_s}$ is about 0.55 emu/cc corresponding to the saturation field of 1.8 kOe, the coercive field $\mathbf{H_c}$ is about 70 Oe and the remanent magnetization $\mathbf{M_r}$ is about 0.085 emu/cc. The calculated squareness of the hysteresis loop is 0.152. Although the magnetization of the nanobraids is weak, the result demonstrates a method to fabricate magnetic nanomaterials. It is believed that the magnetic behaviors would be improved if the concentration of iron is increased.

In summary, based on VLS mechanism, the nanobraids of iron doped silica were fabricated by vapor-phase transport method. SEM, XRD, TEM, and EDX analyses demonstrated the high yield, uniform size amorphous silica nanobraids doped by iron. The nanobraids show a clear ferromagnetic behavior although the iron concentration is low. Apart from potential applications making use of the magnetic properties, these nanobraids may find applications in trapping moistures and vapors.

The sponsorships from Research Grant Manpower Fund (RG51/01) of Nanyang Technological University and Science and Engineering Research Council Grant (No. 0421010010) from Agency for Science, Technology and Research (A*STAR), Singapore are gratefully acknowledged.

[1] S. Iijima, Nature (London) **354**, 56 (1991).
[2] T. W. Odom, J. L. Huang, P. Kim, and C. M. Lieber, Nature (London) **391**, 62 (1998).
[3] Z. R. Dai, Z. W. Pan, and Z. L. Wang, Adv. Funct. Mater. **13**, 9 (2002).
[4] X. Duan, Y. Huang, R. Agarwal, and C. M. Lieber, Nature (London) **421**, 241 (2003).
[5] M. H. Huang, S. Mao, H. Feick, H. Yan, H. Kind, E. Weber, R. Russo, and P. Yang, Science **287**, 465 (2000).
[6] C. X. Xu and X. W. Sun, Appl. Phys. Lett. **83**, 3806 (2003).
[7] C. X. Xu, X. W. Sun, and B. J. Chen, Appl. Phys. Lett. **84**, 1540 (2004).
[8] D. P. Yu, Q. L. Huang, Y. Ding, H. Z. Zhang, Z. G. Bai, J. J. Wang, and Y. H. Zhou, Appl. Phys. Lett. **73**, 3076 (1998).
[9] Z. Q. Liu, S. S. Xie, L. F. Sun, D. S. Tang, W. Y. Zhou, C. Y. Wang, W. Liu, Y. B. Li, X. P. Zhou, and G. Wang, J. Mater. Res. **16**, 683 (2001).
[10] X. C. Wu, W. H. Song, K. Y. Wang, T. Hu, B. Zhao, Y. P. Sun, and J. J. Du, Chem. Phys. Lett. **336**, 53 (2001).
[11] X. S. Peng, X. F. Wang, J. Zhang, Y. W. Wang, S. H. Sun, G. W. Meng, and L. D. Zhang, Appl. Phys. A: Mater. Sci. Process. **74**, 831 (2002).
[12] H. F. Zhang, C. M. Wang, E. C. Buck, and L. S. Wang, Nano Lett. **3**, 577 (2003).
[13] Z. Pan, S. Dai, D. B. Beach, and D. H. Lowndes, Nano Lett. **3**, 1279 (2003).
[14] L. Thomas, F. Lionti, R. Ballou, D. Gatteschi, R. Scssoli, and B. Barhara, Nature (London) **383**, 145 (1996).
[15] K. S. Napolsky, A. A. Eliseev, A. V. Knotko, A. V. Lukahsin, A. A. Vertegel, and Y. D. Tretyakov, Mater. Sci. Eng., C **23**, 151 (2003).
[16] C. Ronning, P. X. Gao, Y. Dong, and Z. L. Wang, Appl. Phys. Lett. **82**, 783 (2004).
[17] Y. C. Wang, J. Ding, J. B. Yi, B. H. Liu, T. Yu, and Z. X. Shen, Appl. Phys. Lett. **84**, 2596 (2004).
[18] M. Wu, Y. D. Zhang, S. Hui, T. D. Xiao, S. Ge, W. A. Hines, and J. I. Budnick, and G. W. Taylor, Appl. Phys. Lett. **80**, 4404 (2002).
[19] H. Guerrero, G. Rosa, M. P. Morales, F. Monte, E. M. Moreno, D. Levy, R. P. Real, T. Belenguer, and C. J. Serna, Appl. Phys. Lett. **71**, 2698 (1997).
[20] C. X. Xu, X. W. Sun, B. J. Chen, P. Shum, S. Li, and X. Hu, J. Appl. Phys. **95**, 661 (2004).
[21] C. H. Liang, L. D. Zhang, G. W. Meng, Y. W. Wang, and Z. Q. Chu, J. Non-Cryst. Solids **277**, 63 (2000).